Hourly Scheduling of DC Transmission Lines in SCUC with Voltage Source Converters

Azim Lotfjou, *Member IEEE,* Mohammad Shahidehpour, *Fellow, IEEE,* Yong Fu, *Member IEEE*[1]

***Abstract*— This paper presents the modeling of high voltage direct current (DC) transmission systems with voltage source converters (VSCs) in security-constrained unit commitment (SCUC). The impact of VSC-DC transmission system on the economics and the security of integrated AC/DC transmission systems is discussed. The nonlinear AC/DC equations are linearized and the Newton-Raphson method is utilized to solve the linearized network in the base case and contingencies. The SCUC solution will determine the optimal hourly schedule of controllable VSC-DC transmission systems in electricity markets. Numerical examples show the efficiency of the proposed model.**

Keywords: *high voltage direct current transmission lines, voltage source converters, security-constrained unit commitment,*

NOMENCLATURE

b Index of AC buses
c Superscript for contingency
NB Number of AC buses
E_h AC side voltage of the converter h
h Index of DC converters
i Index of units
t Index of hour
inj Superscript for an injection
$I_{dc,h}$ DC current of converter h
U_{it} on/off state of generating unit i at time t
$\hat{U}_{it}$, $\hat{P}_{it}$ State and generation dispatch solution of unit i at time t
l Index of lines
m Index of AC bus terminals connected with converters
max, min Subscript for maximum and minimum values
M_h Modulation index of converter h
P_{it} Generation dispatch of unit i at time t
P_h DC active power through converter h
P_m Withdrawal real power at ac bus m
$P_{term,h}$ Active power injected into the converter h
Q_h DC reactive power through the converter h
Q_m Withdrawal reactive power at AC bus m
$Q_{term,h}$ Reactive power injected into converter h
R_{dc} Resistance of DC line
$SP1_b$, $SP2_b$ Slack variables for real power mismatch at bus b (>=0)
$SQ1_b$, $SQ2_b$ Slack variables for reactive power mismatch at bus b (>=0)
w Objective of SCUC subproblem
X_h Leakage reactance of coupling transformer connected to converter h
V_m AC voltage at bus m
$V_{dc,h}$ DC voltage of converter h
ϕ_h Power factor lagging/leading angle of converter h ($0 \le \phi_h \le \frac{\pi}{2}$ for rectifier, $-\frac{\pi}{2} \le \phi_h \le 0$ for inverter)
ΔP_m, ΔQ_m Active and reactive power mismatch at ac bus m
$\Delta R1_h$ $\Delta R2_h$, $\Delta R3_h$ Mismatches of DC power flow equations related to converter h
Δ_i Permissible real power adjustment for unit i
$\mathbf{A}$ Bus-unit incidence matrix
$\mathbf{G}_h$ Admittance matrix of DC network for converters h
$\mathbf{U}$ Generating unit state vector (0 or 1 values)
$\hat{\mathbf{U}}$, $\hat{\mathbf{P}}$ Generating unit state and economic dispatch solutions
$\mathbf{I_{dc}}$, $\mathbf{\Delta I_{dc}}$ Vector of DC current and its increment vector
$\mathbf{J1}$, $\mathbf{J2}$, $\mathbf{J3}$, $\mathbf{J4}$, $\mathbf{J5}$, $\mathbf{J6}$ Jacobian matrices
$\mathbf{M}$, $\mathbf{\Delta M}$ Modulation index vector and its increment vector
$\mathbf{M_0}$ Initial modulation index vector
$\mathbf{MP1}$, $\mathbf{MP2}$, $\mathbf{MQ1}$, $\mathbf{MQ2}$ Mismatch vectors
$\mathbf{P}$, $\mathbf{Q}$ Vector of real and reactive power generation of units
$\mathbf{V}$, $\mathbf{V_{dc}}$ AC and DC bus voltage vectors
$\mathbf{E}$, $\mathbf{\Delta E}$ Vector for AC side voltage of converters and its increment vectors
$\boldsymbol{\varphi}$, $\boldsymbol{\Delta\varphi}$ Power factor angle vector and its increment vector
$\boldsymbol{\delta}$, $\boldsymbol{\Delta\delta}$ Bus phase angle vector and its increment vector
$\mathbf{dP_0}$ Initial AC bus real power mismatch vector
$\mathbf{dQ_0}$ Initial AC bus reactive power mismatch vector
$\mathbf{dR1_0}$, $\mathbf{dR2_0}$, $\mathbf{dR3_0}$ Initial mismatch vectors of DC equations
π, $\underline{\psi}$, $\overline{\psi}$ Simplex multipliers vectors
$\mathbf{\Delta PL_{ac}}$, $\mathbf{\Delta PL_{dc}}$ Vector of AC and DC line flow Increments
$\mathbf{\Delta T}$ Vector of transformer tap increment
$\mathbf{\Delta\gamma}$ Vector of phase-shifter angle increment

I. INTRODUCTION

Modern power systems introduce VSC-DC transmission systems to enhance the operation and the flexibility of AC transmission systems in electricity markets. VCS-DC transmission systems use insulated gate bipolar transistors (IGBTs) for transmitting remote energy resources reliably and economically to load centers [1-3]. VSC-DC links use pulse

[1] Azim Lotfjou and Mohammad Shahidehpour are with the ECE Department at Illinois Institute of Technology. Yong Fu is with the ECE Department at Mississippi State University. This work was supported in part by the U.S. Department of Energy Grants # DE-EE 0001380.000 and DE-EE 0002979.
.

width modulation (PWM) to set firing angles of IGBT switches in order to offer high speed controls.

In contrast to current source converter (CSC-DC) systems, VSC-DC transmission systems allow rapid and independent control of active and reactive power flows in all four quadrants by changing PWM firing patterns. VSC-DC transmission systems provide a full control to turn on/off IGBT switches for regulating DC voltages and power factors instantaneously and providing continuous and dynamic voltage regulations at AC transmission systems. Unlike CSCs, VSCs would not require active voltage commutations to switch off IGBTs, which enables them to feed isolated AC loads [4, 5]. Recently, VSC-DC taps were introduced to deliver energy to small loads located in the vicinity of DC lines [6, 7].

VSC-DC transmission systems were modeled as back-to-back links or similar configurations in power flow analyses [8-11]. Such studies utilized the Newton-Raphson method to solve nonlinear VCS-DC power flow equations. Two control actions, i.e., constant active power plus constant DC voltage (PV) and constant active power plus constant reactive power (PQ) were defined to maintain the secure operation of VSC-DC transmission systems. Also VSC-DC transmission constraints were included in the optimal power flow formulation by assuming that the total active power injection to a VSC-DC link was equal to power losses in the link.

In contrast to numerous publications on the modeling of phase shifters and FACTS devices in electricity markets [12-13], few studies investigated the optimal control of VSC-DC transmission systems in electricity markets. In this paper, we analyze the control and the scheduling of multi-terminal VSC-DC transmission systems and provide the optimal schedule for the control of VSC-DC transmission systems in the base case and contingencies.

We include the VSC-DC model in SCUC. As one of key tools for market clearing, the SCUC solution will provide the optimal hourly schedule of generating units and the optimal schedule of VSC-DC transmission systems for enhancing the security and economics. This paper uses sequential linear programming to find a feasible solution to the SCUC subproblem which may not guarantee a global optimal solution.

The rest of this paper is organized as follows. Section II discusses the DC modeling. The SCUC integrated with DC systems is presented in section III. The proposed model is tested with a 6-bus system and the IEEE 118-Bus system in section IV. We summarize our conclusion in section V.

II. VSC-DC MODEL

A. VSC-DC Transmission Model

We assume a balanced three phase conditions. In order to model the VSC h which is connected to the AC terminal's bus m, five variables including the direct voltage $V_{dc,h}$, direct current $I_{dc,h}$, converter AC voltage E_h, PWM modulation index M_h and the lagging/leading power factor angle φ_h, are defined in Fig. 1 [4]. E_h is controlled by adjusting M_h as

$$\begin{cases} E_h = \dfrac{M_h}{2\sqrt{2}} V_{dc,h} & \text{for rectifier} \\ E_h = -\dfrac{M_h}{2\sqrt{2}} V_{dc,h} & \text{for inverter} \end{cases} \quad (1)$$

where $0 \le M_h \le 1$. Also $P_{term,h}$ is controlled by adjusting φ_h,

$$\begin{cases} P_{term,h} = \dfrac{V_m E_h \sin(\varphi_h)}{X_h} & \text{for rectifier} \\ P_{term,h} = -\dfrac{V_m E_h \sin(\varphi_h)}{X_h} & \text{for inverter} \end{cases} \quad (2)$$

where $0 \le \phi_h \le \dfrac{\pi}{2}$ for rectifiers and $-\dfrac{\pi}{2} \le \phi_h \le 0$ for inverters. Assuming converter transformers, valves, and DC capacitors are lossless, the active power converted into DC is

$$P_{term,h} = P_h = V_{dc,h} I_{dc,h} \quad (3)$$

Combining (1)-(3), we obtain the second converter equation as

$$\begin{cases} I_{dc,h} = \dfrac{M_h V_m \sin(\varphi_h)}{2\sqrt{2} X_h} & \text{for rectifier} \\ I_{dc,h} = -\dfrac{M_h V_m \sin(\varphi_h)}{2\sqrt{2} X_h} & \text{for inverter} \end{cases} \quad (4)$$

The VSC in Fig. 1 generates $-Q_h$, where

$$Q_h = -\frac{E_h (E_h - V_m \cos(-\varphi_h))}{X_h} \quad (5)$$

The reactive power flow from bus m to VSC-DC link is

$$Q_{term,h} = \frac{V_m (V_m - E_h \cos(\varphi_h))}{X_h} \quad (6)$$

The difference between $Q_{term,h}$ and Q_h is the reactive power loss in the coupling transformer series reactance [14].

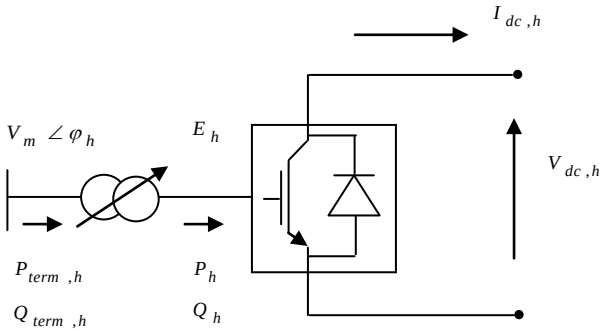

Fig 1. Schematic diagram of a VSC

B. DC Transmission Line Model

In this paper, we model two-terminal DC transmission systems based on the converter model presented in section III.A. However, mathematical derivations can be easily expanded to any DC configurations with any number of VSCs. In Fig. 2, two VSCs are connected to AC buses $m1$ and $m2$ via coupling transformers. We assume that the converter $h1$ is a rectifier and converter $h2$ operates as an inverter. Converters $h1$ and $h2$ are connected by a DC transmission line with a resistance R_{dc}. Here, (7) represents the model for a two-terminal DC configuration

$$\begin{bmatrix} I_{dc,h1} \\ I_{dc,h2} \end{bmatrix} = \begin{bmatrix} \frac{1}{R_{dc}} & \frac{1}{R_{dc}} \\ \frac{1}{R_{dc}} & \frac{1}{R_{dc}} \end{bmatrix} \begin{bmatrix} V_{dc,h1} \\ V_{dc,h2} \end{bmatrix} \quad (7)$$

For a multi-terminal DC system, the equation in matrix form is

$$\mathbf{I_{dc}} = \mathbf{G.V_{dc}} \quad (8)$$

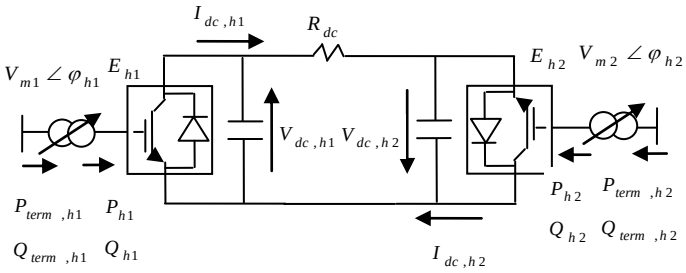

Fig 2. Schematic of a two-terminal VSC-DC system

C. Control Modes of DC Transmission

DC links have two control modes including PV and PQ at their converter stations. In the PV control mode (9), VSC sets P_h and E_h at a specified level, while the PQ control mode (10) will keep a constant active power flow and reactive power flow. In each VSC-DC transmission link, at least one converter would operate in the PV mode to adjust DC voltages while others operate in PV or PQ mode.

$$P_h - P_h^{spec} = 0, \quad E_h - E_h^{spec} = 0 \quad (9)$$

$$P_h - P_h^{spec} = 0, \; Q_h - Q_h^{spec} = 0 \quad (10)$$

The PV control is used in VSC-DC transmission links to secure the transfer of scheduled active power while maintaining AC voltages against possible disturbances. VSC-DC injects a specific amount of reactive power into the AC system for satisfying reactive power requirements and increasing the available transfer capacity (ATC) of AC system in the PQ control mode. In this paper, we consider upper and lower limits of control variables for the optimal control of VSC-DC system in the SCUC solution.

A back-to-back VSC-DC link that connects two AC systems would have one station for both rectifier and inverter systems with a zero DC line resistance. In back-to-back VSC-DC systems, (11) and (12) will replace (3) and (8), respectively.

$$P_{h1} = P_{h2} \quad (11)$$

$$V_{dc,h1} = V_{dc,h2} \quad (12)$$

D. VSC-DC Power Flow Equations

The nodal power balance at bus *m* which is connected to converter *h* is given as

$$\Delta P_m = P_m^{inj} - P_m - P_{term,h} = 0 \quad (13)$$

$$\Delta Q_m = Q_m^{inj} - Q_m - Q_{term,h} = 0 \quad (14)$$

where, $P_{term,h} = V_{dc,h} I_{dc,h}$ and $Q_{term,h} = \frac{V_m (V_m - E_h \cos(\varphi_h))}{X_h}$

The power flow in per-unit for converter *h* at the AC terminal bus *m* is given as

$$\begin{cases} \Delta R1_h = E_h - \frac{M_h}{2\sqrt{2}} V_{dc,h} = 0 & \text{for rectifier} \\ \Delta R1_h = E_h + \frac{M_h}{2\sqrt{2}} V_{dc,h} = 0 & \text{for inverter} \end{cases} \quad (15)$$

$$\begin{cases} \Delta R2_h = I_{dc,h} - \frac{M_h V_m \sin(\varphi_h)}{2\sqrt{2} X_h} = 0 & \text{for rectifier} \\ \Delta R2_h = I_{dc,h} + \frac{M_h V_m \sin(\varphi_h)}{2\sqrt{2} X_h} = 0 & \text{for inverter} \end{cases} \quad (16)$$

$$\Delta R3_h = f(\mathbf{V_{dc}}, I_{dc,h}) = I_{dc,h} - \mathbf{G_h V_{dc}} = 0 \quad (17)$$

III. VSC-DC SYSTEM IN SCUC

Fig. 3 depicts the market clearing algorithm based on SCUC with AC/DC network constraints where market participants in AC systems (i.e., generation companies and customers) submit bids to the independent system operator (ISO). At the same time, transmission companies collect and send AC/DC network data to the ISO. The ISO executes the SCUC to clear the market with AC/DC transmission systems [15] in the base case and contingencies.

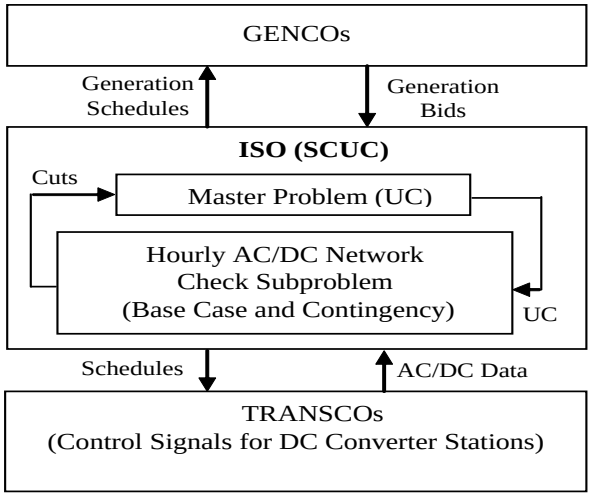

Fig. 3. Market clearing model with AC/DC network constraints

A. SCUC Formulation

The SCUC with integrated AC/DC transmission systems is stated as the following nonlinear optimization problem:

$$\begin{aligned} &Min \quad f(\mathbf{x}) \\ &S.t. \\ &\quad \mathbf{g1(x)} \le \mathbf{b1} \\ &\quad \mathbf{ge1(x)} = \mathbf{be1} \\ &\quad \mathbf{g2(x)} \le \mathbf{b2} \\ &\quad \mathbf{ge2(x)} = \mathbf{be2} \end{aligned} \quad (18)$$

Variable $\mathbf{x}$ represents the on/off status and economic dispatch (ED) of generating units, startup/shut down indicators, and AC/DC control and state variables. The objective is to minimize the operating cost including generation and startup/ shutdown costs. In (18), the first set of inequality constraints, $\mathbf{g1(x)} \le \mathbf{b1}$, and equality constraints, $\mathbf{ge1(x)} = \mathbf{be1}$, represents UC constraints including power balance, generating

unit capacity, system spinning and operating reserve requirements, ramping up/down limits, minimum up/down time limits, maximum number of simultaneous on/offs in a plant, maximum number of on/offs of a generating unit in a given period, fuel and multiple emission limits. The second set of inequality constraints, $\mathbf{g2(x)} \le \mathbf{b2}$, and equality constraints $\mathbf{ge2(x)} = \mathbf{be2}$, include

- AC/DC power flow equations
- Limits on AC/DC control variables including real and reactive power generations, controlled shunt capacitors, tap-changing and phase-shifting transformers, modulation index and converter transformer tap ratios
- AC/DC network security constraints including AC/DC transmission flow and bus voltage limits, and limits to DC currents, voltages and power of converters
- Time limited corrective controls of contingencies such as permissible real power adjustment

B. SCUC Subproblem Formulation in Base Case

DC transmission system constraints are included in the hourly AC/DC network check subproblem which minimizes the AC bus real and reactive power mismatch (19) based on the UC solution while satisfying network security constraints (20)-(35). In essence, AC/DC transmission violations appear as power mismatches at AC buses (20). The hourly subproblem (19)-(35) minimizes slack variables ($MP1$, $MP2$) and ($MQ1$, $MQ2$) which represent the amount of real and reactive power mismatch that should be added to corresponding buses to remove violations. (21) considers DC transmission flows. (22)-(35) represents limits on real and reactive power generations, real and reactive power withdrawals at AC converter terminals, AC and DC transmission flows, AC bus voltage magnitudes, transformer tap settings, phase shifter angles, DC converter voltages and currents, converter modulation index, AC converter voltages and power factor angles. The elements of Jacobian matrices $\mathbf{J1 - J6}$ are calculated in the Appendix A.

$$Min \quad w(\hat{\mathbf{U}}, \hat{\mathbf{P}}) = \sum_{b=1}^{NB} (MP1_b + MP2_b) + (MQ1_b + MQ2_b) \tag{19}$$

s.t.

$$\begin{bmatrix} \mathbf{A} \cdot \Delta\mathbf{P} \\ \mathbf{A} \cdot \Delta\mathbf{Q} \end{bmatrix} - [\mathbf{J1}] \begin{bmatrix} \Delta\boldsymbol{\delta} \\ \Delta\mathbf{V} \\ \Delta\mathbf{T} \\ \Delta\boldsymbol{\gamma} \\ \Delta\mathbf{V}_{\mathbf{dc}} \\ \Delta\mathbf{I}_{\mathbf{dc}} \\ \Delta\mathbf{E} \\ \Delta\boldsymbol{\varphi} \end{bmatrix} + \begin{bmatrix} \mathbf{MP1} \\ \mathbf{MQ1} \end{bmatrix} - \begin{bmatrix} \mathbf{MP2} \\ \mathbf{MQ2} \end{bmatrix} = \begin{bmatrix} \mathbf{dP}_0 \\ \mathbf{dQ}_0 \end{bmatrix} \tag{20}$$

$$-[\mathbf{J2}] \begin{bmatrix} \Delta\mathbf{V} \\ \Delta\mathbf{V}_{\mathbf{dc}} \\ \Delta\mathbf{I}_{\mathbf{dc}} \\ \Delta\mathbf{M} \\ \Delta\mathbf{E} \\ \Delta\boldsymbol{\varphi} \end{bmatrix} = \begin{bmatrix} \mathbf{dR1}_0 \\ \mathbf{dR2}_0 \\ \mathbf{dR3}_0 \end{bmatrix} \tag{21}$$

$$\Delta\mathbf{P} = \mathbf{0} \qquad \boldsymbol{\pi} \tag{22}$$

$$\Delta\mathbf{Q}_{\min} \le \Delta\mathbf{Q} \le \Delta\mathbf{Q}_{\max} \qquad \underline{\boldsymbol{\psi}}, \overline{\boldsymbol{\psi}} \tag{23}$$

$$\Delta\mathbf{P}_{\mathbf{dc,\,min}} \le \Delta\mathbf{P}_{\mathbf{dc}} = [\mathbf{J3}] \begin{bmatrix} \Delta\mathbf{V}_{\mathbf{dc}} \\ \Delta\mathbf{I}_{\mathbf{dc}} \end{bmatrix} \le \Delta\mathbf{P}_{\mathbf{dc,\,max}} \tag{24}$$

$$\Delta\mathbf{Q}_{\mathbf{dc,min}} \le \Delta\mathbf{Q}_{\mathbf{dc}} = [\mathbf{J4}] \begin{bmatrix} \Delta\mathbf{V}_{\mathbf{dc}} \\ \Delta\mathbf{I}_{\mathbf{dc}} \\ \Delta\boldsymbol{\varphi} \end{bmatrix} \le \Delta\mathbf{Q}_{\mathbf{dc,max}} \tag{25}$$

$$\Delta\mathbf{PL}_{\mathbf{ac,min}} \le \Delta\mathbf{PL}_{\mathbf{ac}} = [\mathbf{J5}] \begin{bmatrix} \Delta\boldsymbol{\delta} \\ \Delta\mathbf{V} \\ \Delta\mathbf{T} \\ \Delta\boldsymbol{\gamma} \end{bmatrix} \le \Delta\mathbf{PL}_{\mathbf{ac,max}} \tag{26}$$

$$\Delta\mathbf{PL}_{\mathbf{dc,min}} \le \Delta\mathbf{PL}_{\mathbf{dc}} = [\mathbf{J6}] \begin{bmatrix} \Delta\mathbf{V}_{\mathbf{dc}} \\ \Delta\mathbf{I}_{\mathbf{dc}} \end{bmatrix} \le \Delta\mathbf{PL}_{\mathbf{dc,max}} \tag{27}$$

$$\Delta\mathbf{V}_{\min} \le \Delta\mathbf{V} \le \Delta\mathbf{V}_{\max} \tag{28}$$

$$\Delta\mathbf{T}_{\min} \le \Delta\mathbf{T} \le \Delta\mathbf{T}_{\max} \tag{29}$$

$$\Delta\boldsymbol{\gamma}_{\min} \le \Delta\boldsymbol{\gamma} \le \Delta\boldsymbol{\gamma}_{\max} \tag{30}$$

$$\Delta\mathbf{V}_{\mathbf{dc,min}} \le \Delta\mathbf{V}_{\mathbf{dc}} \le \Delta\mathbf{V}_{\mathbf{dc,max}} \tag{31}$$

$$\Delta\mathbf{I}_{\mathbf{dc,\,min}} \le \Delta\mathbf{I}_{\mathbf{dc}} \le \Delta\mathbf{I}_{\mathbf{dc,\,max}} \tag{32}$$

$$\Delta\mathbf{M}_{\min} \le \Delta\mathbf{M} \le \Delta\mathbf{M}_{\max} \tag{33}$$

$$\Delta\mathbf{E}_{\min} \le \Delta\mathbf{E} \le \Delta\mathbf{E}_{\max} \tag{34}$$

$$\Delta\boldsymbol{\varphi}_{\min} \le \Delta\boldsymbol{\varphi} \le \Delta\boldsymbol{\varphi}_{\max} \tag{35}$$

The optimization of (19)-(35) is described as follows,

1. Initialize AC/DC state variables and settings. For example, $\delta = 0$ rad, $V = 1\ pu$, $V_{dc} = \pm 1\ pu$, $I_{dc} = 0$ amp, $M = 1$, $E = 1\ pu$ and $\varphi = 0$ rad. Calculate corresponding Jacobian matrices $\mathbf{J1 - J6}$, initial AC bus mismatch vectors $\mathbf{dP}_0$ and $\mathbf{dQ}_0$, and initial DC power mismatch $\mathbf{dR1}_0$, $\mathbf{dR2}_0$, $\mathbf{dR3}_0$ based on the given UC solution.
2. Use LP to minimize (19) and calculate changes in AC/DC state and control variables (i.e., $\Delta\boldsymbol{\delta}$, $\Delta\mathbf{V}$, $\Delta\mathbf{T}$, $\Delta\boldsymbol{\gamma}$, $\Delta\mathbf{V}_{\mathbf{dc}}$, $\Delta\mathbf{I}_{\mathbf{dc}}$, $\Delta\mathbf{M}$, $\Delta\mathbf{E}$ and $\Delta\boldsymbol{\varphi}$).
3. Update state and control variables. Recalculate elements of Jacobian matrices and mismatch vectors.
4. Minimize (19) and calculate changes in AC/DC transmission system state and control variables. If the incremental change in objective values within the last two iterations is less than a specified tolerance (i.e., $\mathbf{dR1}, \mathbf{dR2}, \mathbf{dR3} \le \boldsymbol{\varepsilon}$), the DC power flow has converged; stop the iterative process. Otherwise, go back to Step 3.

If $w(\hat{\mathbf{U}}, \hat{\mathbf{P}})$ is larger than zero, ED cannot provide a feasible power flow solution to satisfy AC/DC flow constraints. Hence, a Benders cut (36) will be formed and added to the next iteration of UC problem.

$$w(\mathbf{U}, \mathbf{P}) = w(\hat{\mathbf{U}}, \hat{\mathbf{P}}) + \sum_{i=1}^{NG} (\overline{\pi}_{it} - \underline{\pi}_{it})(P_{it} - \hat{P}_{it}) + \sum_{i=1}^{NG} (\overline{\psi}_{it} Q_{\max,\,i} - \underline{\psi}_{it} Q_{\min,\,i})(U_{it} - \hat{U}_{it}) \le 0 \tag{36}$$

C. Corrective and Preventive Actions for Managing Contingencies

In each contingency, sufficient corrective and preventive actions are considered based on $\left|P_{it} - \hat{P}_{it}^{0}\right| \le \Delta_i$ for managing AC/DC transmission violations [16]. Δ_i is equal to 1/6 of unit *i* hourly ramping which represents the physically accepted adjustment of generating unit in ten minutes. Corrective actions refer to the redispatch of generating units when satisfying transmission flow violations in real time. Preventive actions refer to day-ahead adjustments in the base case UC and ED when considering potential contingencies. Preventive actions cannot be implemented in real time when responding to power flow violations. The hourly AC/DC network check subproblem is formulated as

$$Min \quad w^c(\hat{\mathbf{U}}, \hat{\mathbf{P}}) = \sum_{b=1}^{NB} \left(MP\,1_b^c + MP\,2_b^c + MQ\,1_b^c + MQ\,2_b^c \right) \tag{37}$$

$$\begin{bmatrix} \mathbf{A}\cdot\Delta\mathbf{P}^c \\ \mathbf{A}\cdot\Delta\mathbf{Q}^c \end{bmatrix} - [\mathbf{J1}] \begin{bmatrix} \Delta\boldsymbol{\delta}^c \\ \Delta\mathbf{V}^c \\ \Delta\mathbf{T}^c \\ \Delta\gamma^c \\ \Delta\mathbf{V}_{\mathbf{dc}}^c \\ \Delta\mathbf{I}_{\mathbf{dc}}^c \\ \Delta\mathbf{E}^c \\ \Delta\boldsymbol{\varphi}^c \end{bmatrix} + \begin{bmatrix} \mathbf{MP1}^c \\ \mathbf{MQ1}^c \end{bmatrix} - \begin{bmatrix} \mathbf{MP2}^c \\ \mathbf{MQ2}^c \end{bmatrix} = \begin{bmatrix} \mathbf{dP}_{\mathbf{0}}^c \\ \mathbf{dQ}_{\mathbf{0}}^c \end{bmatrix} \tag{38}$$

$$-[\mathbf{J2}] \begin{bmatrix} \Delta\mathbf{V}^c \\ \Delta\mathbf{V}_{\mathbf{dc}}^c \\ \Delta\mathbf{I}_{\mathbf{dc}}^c \\ \Delta\mathbf{M}^c \\ \Delta\mathbf{E}^c \\ \Delta\boldsymbol{\varphi}^c \end{bmatrix} = \begin{bmatrix} \mathbf{dR1}_{\mathbf{0}}^c \\ \mathbf{dR2}_{\mathbf{0}}^c \\ \mathbf{dR3}_{\mathbf{0}}^c \end{bmatrix} \tag{39}$$

$$\left|\mathbf{P}^c - \hat{\mathbf{P}}^0\right| \le \boldsymbol{\Delta} \qquad \overline{\boldsymbol{\pi}}^c,\ \underline{\boldsymbol{\pi}}^c \tag{40}$$

$$\Delta\mathbf{Q}_{\mathbf{min}}^c \le \Delta\mathbf{Q}^c \le \Delta\mathbf{Q}_{\mathbf{max}}^c \qquad \underline{\boldsymbol{\psi}}^c,\ \overline{\boldsymbol{\psi}}^c \tag{41}$$

$$\Delta\mathbf{P}_{\mathbf{dc,\,min}}^c \le \Delta\mathbf{P}_{\mathbf{dc}}^c \le \Delta\mathbf{P}_{\mathbf{dc,\,max}}^c \tag{42}$$

$$\Delta\mathbf{Q}_{\mathbf{dc,\,min}}^c \le \Delta\mathbf{Q}_{\mathbf{dc}}^c \le \Delta\mathbf{Q}_{\mathbf{dc,\,max}}^c \tag{43}$$

$$\Delta\mathbf{PL}_{\mathbf{ac,\,min}}^c \le \Delta\mathbf{PL}_{\mathbf{ac}}^c \le \Delta\mathbf{PL}_{\mathbf{ac,\,max}}^c \tag{44}$$

$$\Delta\mathbf{PL}_{\mathbf{dc,\,min}}^c \le \Delta\mathbf{PL}_{\mathbf{dc}}^c \le \Delta\mathbf{PL}_{\mathbf{dc,\,max}}^c \tag{45}$$

$$\Delta\mathbf{V}_{\mathbf{min}}^c \le \Delta\mathbf{V}^c \le \Delta\mathbf{V}_{\mathbf{max}}^c \tag{46}$$

$$\Delta\mathbf{T}_{\mathbf{min}}^c \le \Delta\mathbf{T}^c \le \Delta\mathbf{T}_{\mathbf{max}}^c \tag{47}$$

$$\Delta\gamma_{\mathbf{min}}^c \le \Delta\gamma^c \le \Delta\gamma_{\mathbf{max}}^c \tag{48}$$

$$\Delta\mathbf{V}_{\mathbf{dc,\,min}}^c \le \Delta\mathbf{V}_{\mathbf{dc}}^c \le \Delta\mathbf{V}_{\mathbf{dc,\,max}}^c \tag{49}$$

$$\Delta\mathbf{I}_{\mathbf{dc,\,min}}^c \le \Delta\mathbf{I}_{\mathbf{dc}}^c \le \Delta\mathbf{I}_{\mathbf{dc,\,max}}^c \tag{50}$$

$$\Delta\mathbf{M}_{\mathbf{min}}^c \le \Delta\mathbf{M}^c \le \Delta\mathbf{M}_{\mathbf{max}}^c \tag{51}$$

$$\Delta\mathbf{E}_{\mathbf{min}}^c \le \Delta\mathbf{E}^c \le \Delta\mathbf{E}_{\mathbf{max}}^c \tag{52}$$

$$\Delta\boldsymbol{\varphi}_{\mathbf{min}}^c \le \Delta\boldsymbol{\varphi}^c \le \Delta\boldsymbol{\varphi}_{\mathbf{max}}^c \tag{53}$$

The objective function (37) is introduced for minimizing real and reactive power mismatches when calculating a converged power flow solution subject to transmission flow and bus voltage limits. If $w^c(\hat{\mathbf{U}}, \hat{\mathbf{P}})$ is larger than zero, a Benders cut (54) for contingency c will be formed and added to UC for calculating the next iterative solution of master problem.

$$w^c(\hat{\mathbf{U}}, \hat{\mathbf{P}}) = \boldsymbol{\pi}^c(\mathbf{P} - \hat{\mathbf{P}}^0) + \overline{\boldsymbol{\psi}}^c\mathbf{Q}_{\max}(\mathbf{U} - \hat{\mathbf{U}}^0) - \underline{\boldsymbol{\psi}}^c\mathbf{Q}_{\min}(\mathbf{U} - \hat{\mathbf{U}}^0) \le 0 \tag{54}$$

IV. Numerical Examples

We study a six bus system and a modified IEEE-118 bus system in the base case and contingencies.

A. Six-bus System

The six-bus system shown in Fig. 4 has three generating units, seven AC transmission lines, two transformers and three loads. The slack bus is bus 1.

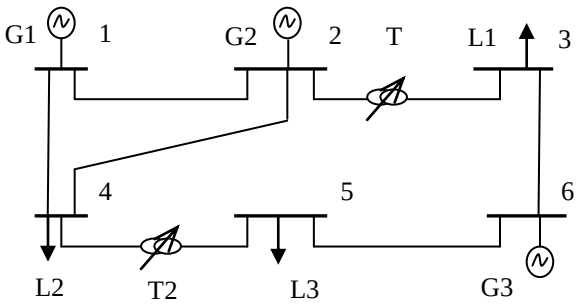

Fig. 4. Schematic diagram of six-bus system

The system data are presented in Appendix B. The following seven cases are tested in which Case 0 is for the UC problem (Base Case), Cases 1-3 consider SCUC with network constraints, and Cases 4-6 evaluate contingencies.

Case 0: UC without transmission constraints

Case 1: SCUC with AC transmission constraints

Case 2: SCUC with AC/DC transmission constraints in which the AC line 1-2 is replaced with a VSC-DC transmission link

Case 3: SCUC with AC/DC transmission constraints in which the AC line 1-2 is replaced with a CSC-DC transmission link.

Case 4: SCUC for Case 1 when the possible outage of unit 3 (CTGU3) is considered (preventive contingency)

Case 5: SCUC for Case 2 when the possible outage of unit 3 (CTGU3) is considered (corrective contingency)

Case 6: SCUC for Case 3 when the possible outage of unit 3 (CTGU3) is considered (corrective contingency)

In each case, base case and contingencies are considered to evaluate the system security and economics in different operating conditions. The results are presented as follows.

Case 0: When transmission constraints are ignored, the cheapest unit 1 will pick up the hourly base load and the more expensive unit 2 will be committed at hours 11-22 to supply partial loads. In this case, the most expensive unit 3 is not committed. The hourly UC is shown in Table I with a daily operating cost of $108,240.73.

Case 1: When AC transmission constraints are considered based on the UC solution in Case 0, we find power flow violations at hours 1 and 7-24. Accordingly, 19 Benders cuts at

violated hours are generated and added to the master problem for the next UC calculation. After four SCUC iterations, all violations are removed and the final UC results are shown in Table II in which the changes in comparison to Case 0 are presented in bold. Unit 2 was committed at hour 1, and though there is no violation at hour 2, unit 2 with a minimum on/off time of 2 hours will remain committed at hour 2. The total operating cost is $118,856.15.

TABLE I
UC RESULTS IN CASE 0

	Total Operation Cost = $108240.73
Unit	**Hours (1-24)**
1	1 1 1 1 1 1 1 1 1 1 1 1 1 1 1 1 1 1 1 1 1 1 1 1
2	0 0 0 0 0 0 0 0 0 0 0 1 1 1 1 1 1 1 1 1 1 1 0 0
3	0 0 0 0 0 0 0 0 0 0 0 0 0 0 0 0 0 0 0 0 0 0 0 0

TABLE II
UC RESULTS IN CASE 1

	Total Operation Cost = $ 118856.15
Unit	**Hours (1-24)**
1	1 1 1 1 1 1 1 1 1 1 1 1 1 1 1 1 1 1 1 1 1 1 1 1
2	**1 1** 0 0 0 0 **1 1 1 1** 1 1 1 1 1 1 1 1 1 1 **1 1**
3	0 0 0 0 0 0 0 0 0 0 **1 1 1 1 1 1 1 1 1 1 1 1** 0 0

TABLE III
UC RESULTS IN CASE 2

	Total Operation Cost = $ 113678.76
Unit	**Hours (1-24)**
1	1 1 1 1 1 1 1 1 1 1 1 1 1 1 1 1 1 1 1 1 1 1 1 1
2	**0 0** 0 0 0 0 0 0 **0 0 0 0** 1 1 1 1 1 1 1 1 **0 0 0**
3	0 0 0 0 0 0 0 0 0 0 0 1 1 1 1 1 1 1 1 1 1 0 0

Case 2: SCUC with AC/DC transmission constraints is calculated when the AC line 1-2 is replaced with a VSC-DC link with R_{dc}= 0.005 pu. We find power flow violations at hours 11-22 based on UC results in Case 0. Hence, 11 cuts are generated by (36) and added to the next UC calculation. All AC/DC violations are removed after three SCUC iterations. The final hourly UC is shown in Table III in which changes in comparison to Case 1 are presented in bold. In this case, the VSC-DC link transfers the additional generation of unit G1 from bus 1 to bus 2. For example, 141 MW flow on the DC transmission line 1-2 in this case is compared to 52.75 MW flow on the AC line 1-2 in Case 1 at hour 17. Consequently, the cheaper unit 1 generates 220 MW at peak hour 17 while it generated only 132.16 MW in Case 1. The expensive unit 2 is off at hours 1-2, 9-12 and 22-24 and the total operating cost is $113,678.76 which is less than that in Case 1. Tables IV and V show the optimal operating points of rectifier and inverter over 24 hours, respectively. The optimal control strategy of DC transmission line is determined according to the values in Tables IV and V. For instance, based on control criteria presented in section III.C, at hour 21, the rectifier will have a PV control mode ($P = 141.46\ MW$ plus $V = 1.20\ pu$) and the inverter will have a PQ control mode ($P = -140.76\ MW$ plus $Q = -70\ MVar$). For a two-terminal VSC-DC system, at least one converter should maintain the DC voltage.

Case 3: In this case, the SCUC solution with AC/DC transmission constraints is calculated in which the AC line 1-2 is replaced with a CSC-DC transmission link shown in Fig. 5. α and T are the firing/extinction angle and the transformer

TABLE IV
RECTIFIER OPERATING POINT IN CASE 2

Hour	**P_{term} (MW)**	**Q_{term} (MVAR)**	**V_{dc} (pu)**	**I_{dc} (pu)**	**M (pu)**	**E (pu)**
1	100.91	-50.36	1.20	0.84	0.87	1.05
2	90.75	15.79	1.17	0.77	0.81	0.95
3	84.18	11.10	1.20	0.70	0.83	1.00
4	80.16	44.93	1.20	0.67	0.91	1.09
5	80.51	40.89	1.20	0.67	0.86	1.03
6	85.99	66.71	1.20	0.72	0.84	1.01
7	99.13	-55.69	1.16	0.85	0.90	1.05
8	103.32	-52.05	1.17	0.88	0.82	0.96
9	112.53	29.68	1.20	0.94	0.90	1.08
10	132.91	30.53	1.20	1.11	0.90	1.08
11	141.19	-31.28	1.16	1.22	0.85	0.98
12	141.28	-15.45	1.15	1.23	0.86	0.98
13	141.28	-52.82	1.20	1.18	0.85	1.02
14	141.34	-36.60	1.20	1.18	0.90	1.08
15	141.25	-36.07	1.20	1.18	0.92	1.11
16	141.26	-55.41	1.20	1.18	0.90	1.08
17	141.00	-55.45	1.20	1.18	0.90	1.08
18	141.03	-50.61	1.20	1.18	0.85	1.02
19	141.06	-40.97	1.17	1.20	0.84	0.99
20	141.19	-41.55	1.20	1.18	0.81	0.98
21	141.46	-41.56	1.20	1.18	0.81	0.98
22	141.88	6.97	1.17	1.21	0.83	0.97
23	121.77	41.63	1.20	1.01	0.87	1.05
24	121.41	1.39	1.20	1.01	0.91	1.09

TABLE V
INVERTER OPERATING STATUS IN CASE 2

Hour	**P_{term} (MW)**	**Q_{term} (MVAR)**	**V_{dc} (pu)**	**I_{dc} (A)**	**M (pu)**	**E (pu)**
1	-100.56	-20.63	-1.20	0.84	0.76	0.90
2	-90.45	-48.97	-1.17	0.77	0.80	0.94
3	-83.94	-63.26	-1.20	0.70	0.89	1.06
4	-79.93	-38.51	-1.20	0.67	0.90	1.08
5	-80.29	-41.14	-1.20	0.67	0.86	1.03
6	-85.73	-51.33	-1.20	0.72	0.87	1.04
7	-98.76	-18.95	-1.16	0.85	0.78	0.90
8	-102.93	-65.01	-1.17	0.88	0.84	0.99
9	-112.09	-53.62	-1.20	0.94	0.90	1.08
10	-132.30	-54.52	-1.19	1.11	0.89	1.06
11	-140.44	-70.00	-1.15	1.22	0.83	0.96
12	-140.52	-70.00	-1.14	1.23	0.84	0.96
13	-140.58	-70.00	-1.19	1.18	0.80	0.95
14	-140.65	-32.17	-1.19	1.18	0.77	0.92
15	-140.56	-70.00	-1.19	1.18	0.91	1.08
16	-140.57	-70.00	-1.19	1.18	0.87	1.04
17	-140.30	-70.00	-1.19	1.18	0.87	1.04
18	-140.34	-70.00	-1.19	1.18	0.80	0.96
19	-140.34	-70.00	-1.17	1.20	0.83	0.96
20	-140.50	-70.00	-1.19	1.18	0.81	0.96
21	-140.76	-70.00	-1.19	1.18	0.81	0.96
22	-141.14	-70.00	-1.17	1.21	0.82	0.96
23	-121.25	-58.17	-1.19	1.01	0.88	1.05
24	-120.90	-58.20	-1.19	1.01	0.91	1.09

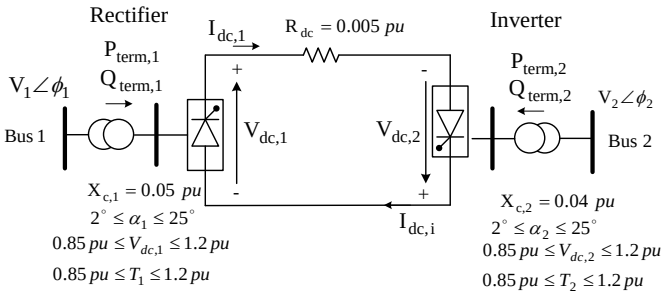

Fig. 5. Schematic diagram of the two-terminal CSC-DC link

tap ratio of rectifier/inverter terminals respectively. Similar to the VSC-DC transmission system, the CSC-DC system can have full control over its real power transmission.

Tables VI and VII show the operating status of CSC-DC transmission system over 24 hours. Comparing Cases 2 and 3, we learn that VSC-DC and CSC-DC systems would change the direction of real power flow to mitigate congestions. Here, P_{term} in Tables IV and VI or Tables V and VII are quite similar. However, the CSC-DC transmission system consumes reactive power during the AC to DC power conversion (non-positive Q_{term} in Tables VI and VII). Since the corresponding voltage profile is degraded, we would create additional cuts for voltage violations. Here, generating unit 2 is committed at hours 1-12, 22-24 to supply the reactive power for keeping the AC voltage at bus 2 within its limits. Table VIII shows that the expensive unit 3 is not committed at these hours when generating units 1 and 2 with a minimum on time of 2 hours will satisfy network constraints at hours 11 and 22 (compared with UC results presented in Table III). The total operating cost is $116,980.07 which is higher than that in Case 2.

TABLE VI
RECTIFIER OPERATION STATUS IN CASE 3

Hour	P_{term} (MW)	Q_{term} (MVAR)	V_{dc} (pu)	I_{dc} (A)	α (Deg)	T (pu)
1	93.84	23.52	1.17	257.25	4.04	1.10
2	85.30	20.68	1.13	242.87	2	1.06
3	82.32	21.39	1.08	244.54	4.31	1.08
4	74.93	19.65	0.99	243.54	2	1.01
5	74.59	18.00	1.06	225.37	2	1.05
6	80.05	18.73	1.13	228.23	2	1.06
7	94.04	23.10	1.17	257.92	2	1.10
8	99.09	25.17	1.17	272.46	2	1.10
9	108.22	28.46	1.18	293.43	2	1.12
10	96.99	24.28	1.17	266.14	2	1.10
11	81.64	18.72	1.16	226.59	2	1.08
12	94.33	23.13	1.17	257.86	2	1.10
13	88.77	21.16	1.17	244.18	2	1.10
14	87.30	20.64	1.17	240.43	2	1.09
15	82.97	19.13	1.16	229.45	2	1.09
16	78.02	17.46	1.15	217.00	2	1.08
17	77.83	17.41	1.15	216.61	2	1.08
18	84.65	19.70	1.16	233.62	2	1.09
19	85.29	19.94	1.16	235.36	2	1.09
20	93.20	22.72	1.17	255.03	2	1.10
21	93.24	22.74	1.17	255.13	2	1.10
22	77.60	17.35	1.15	216.19	2	1.08
23	54.03	10.19	1.10	157.07	2	1.05
24	103.83	26.89	1.18	283.64	2	1.11

Case 4: When the possible outage of unit 3 is considered (CTGU3), the UC results obtained in Case 1 for base case cannot supply the hourly load at hours 1-2 and 6-24. The hourly AC/DC network check subproblem solution presented in (37)-(53) generates Benders cuts related to existing violations for CTGU3. The final UC results presented in Table IX shows that this contingency is uncontrollable and preventive actions (i.e., additional commitment of unit 2 at hour 6) are necessary to maintain the system security in base case and contingency cases. In Table IX, commitment changes in comparison with Table II are shown in bold.

Case 5: Based on UC results obtained in Case 2, the system state can transfer to the base case by applying corrective actions (i.e., redispatch of units 1-2 and adjustments of phase-shifter angles, transformers tap ratios, and VSC controls). The total operating cost increases to $119456.27. In essence, $119456.27-$113678.76=$5777.51 is the cost of maintaining the system security in the event of CTGU3.

TABLE VII
INVERTER OPERATION STATUS IN CASE 3

Hour	P_{term} (MW)	Q_{term} (MVAR)	V_{dc} (pu)	I_{dc} (A)	α (Deg)	T (pu)
1	-93.52	23.75	1.17	257.25	2	1.17
2	-85.01	21.33	1.12	242.87	2	1.13
3	-82.03	21.22	1.08	244.54	2	1.16
4	-74.64	20.23	0.98	243.54	2	1.06
5	-74.34	21.36	1.06	225.37	8.29	1.16
6	-79.80	24.49	1.12	228.23	10.54	1.14
7	-93.72	23.82	1.17	257.92	2	1.17
8	-98.73	26.08	1.16	272.46	2.26	1.17
9	-107.80	29.75	1.18	293.43	3.07	1.19
10	-96.64	25.31	1.17	266.14	2.95	1.19
11	-81.39	19.26	1.15	226.59	2	1.19
12	-94.01	23.87	1.17	257.86	2	1.19
13	-88.48	21.81	1.16	244.18	2	1.19
14	-87.02	21.26	1.16	240.43	2	1.19
15	-82.72	19.68	1.16	229.45	2	1.19
16	-77.79	17.95	1.15	217.00	2	1.19
17	-77.60	17.89	1.15	216.61	2	1.19
18	-84.39	20.28	1.16	233.62	2	1.19
19	-85.02	20.53	1.16	235.36	2	1.19
20	-92.89	23.44	1.17	255.03	2	1.19
21	-92.92	23.45	1.17	255.13	2	1.19
22	-77.37	17.83	1.15	216.19	2	1.19
23	-53.91	10.42	1.10	157.07	2	1.16
24	-103.44	28.42	1.17	283.64	4.3528	1.19

TABLE VIII
UC RESULTS IN CASE 3

	Total Operation Cost = $ 116980.07
Unit	**Hours (1-24)**
1	1 1 1 1 1 1 1 1 1 1 1 1 1 1 1 1 1 1 1 1 1 1 1 1
2	**1 1 1 1 1 1 1 1 1 1 1 1** 1 1 1 1 1 1 1 1 1 **1 1 1**
3	0 0 0 0 0 0 0 0 0 0 **0** 1 1 1 1 1 1 1 1 1 1 **0** 0 0

TABLE IX
UC RESULTS IN CASE 4

	Total Operation Cost = $ 118856.15
Unit	**Hours (1-24)**
1	1 1 1 1 1 1 1 1 1 1 1 1 1 1 1 1 1 1 1 1 1 1 1 1
2	1 1 0 0 0 **1** 1 1 1 1 1 1 1 1 1 1 1 1 1 1 1 1 1
3	0 0 0 0 0 0 0 0 0 0 0 1 1 1 1 1 1 1 1 1 1 1 0 0

Case 6: Based on the UC results in Case 3, the system state cannot be transferred to another base case state in the event of CTGU3. In other word, the system does not have a sufficient supply of reactive power for satisfying the hourly load while maintaining the system security. The system operator would resort to load shedding in the event of CTGU3 to find a SCUC solution. The provision of additional reactive power would guarantee a feasible SCUC solution.

B. IEEE-118 Bus System

A modified IEEE 118–bus system shown in Fig. 6 is tested. This system has 54 units, 186 branches, 14 capacitors, 9 tap-changing transformers and 91 demand sides. Zones 1 and 3 are connected by the AC tie line 23-24. Zones 2 and 3 are connected by AC tie lines 47-69, 49-69, and 65-68. In this example, we study the system performance for five cases. These cases include three zones which are operating

independently, interconnected with AC tie lines, or with VSC-DC lines. In each case, the system security is examined in different operating conditions. Furthermore, this example highlights the salient characteristics of VSC-DC transmission systems for enhancing the system security and economics. The 118-bus system data are given in http://motor.ece.iit.edu/DC/ VSC/ IEEE118.xls. The following cases are tested.

Case 0: UC for three separate zones (without flow constraints)

Case 1: UC for the entire system (without flow constraints)

Case 2: SCUC when three zones are connected by AC lines

Case 3: SCUC when three zones are connected by DC lines

Case 4: SCUC for Case 2 when the possible outage of unit 47 at Zone 2 is considered (preventive contingency)

Case 5: SCUC for Case 3 when the possible outage of unit 47 at Zone 2 is considered (corrective contingency)

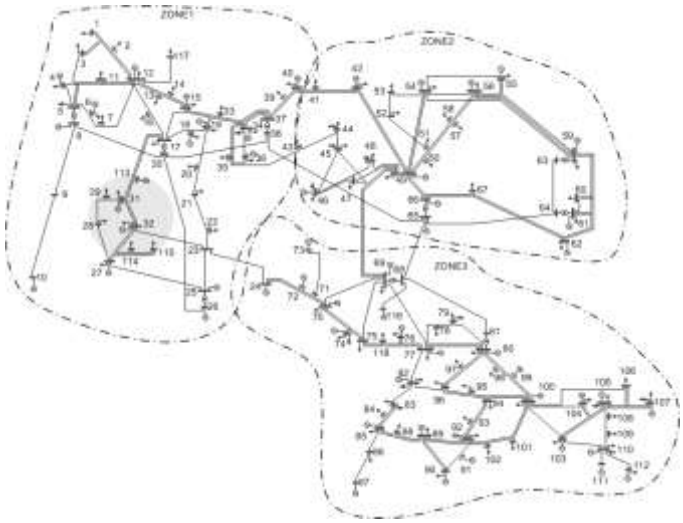

Fig. 6. Schematic diagram of IEEE 118-bus system

The details are given as follows.

Case 0: Since the generation in Zone 1is insufficient for supplying the load, the UC solution for this zone does not converge. In fact, Zone 1 imports power from the other two zones to supply its hourly load economically. The UC solutions converge in Zones 2 & 3 with a total operating cost of $496,426.1 and $659,534.06, respectively.

Case 1: In this case, the generation capacity in the 118-bus network is sufficient for supplying the hourly load. The final UC solution has a total operating cost of $1,727,165.

Case 2: The UC solution in Case 1 are used to analyze SCUC using (19)-(35). Accordingly, certain transmission violations occur which include peak-hour reactive power shortages at buses 21, 41 and 86. These three buses are PQ buses that would need the additional reactive power supply to keep their bus voltages within acceptable limits. Consequently, more expensive units are committed which increase the operating cost to $1,730,600.

Case 3: In this case, we replace AC tie lines with VSC-DC tie lines. We assume that converter terminals are similar to those listed in Table B.VI. Applying the UC results in Case 1, we find that there are violations at hours 1-7, 10-11, 14-16, and 18-23. Consequently, Benders cuts are generated using (36) and a new UC solution is calculated. The total operating cost is $1,728,242 that is less than that in Case 2. In this Case, the VSC-DC transmission system provides three additional degrees of flexibility (i.e., P, Q, and V) for security and economics. Consider AC and DC tie flows in Fig. 7 which represent the peak hour 17. The optimal loading will increase when the AC tie line 65-68 (in Case 2) is replaced with the DC tie line. The economical flows of other DC tie lines are adjusted similarly to minimize the total operating cost while enhancing the security margins in the base case. In other word, the DC control will optimize power exchanges among the three Zones. Table X compares the zonal operating costs at base case (Cases 0-3). Here, the operating costs in Zones 2&3 have increased in Case 3 as compared with that of Case 2; however, the total cost in this case is lower than that of Case 2 because of cost savings provided by Zone 1.

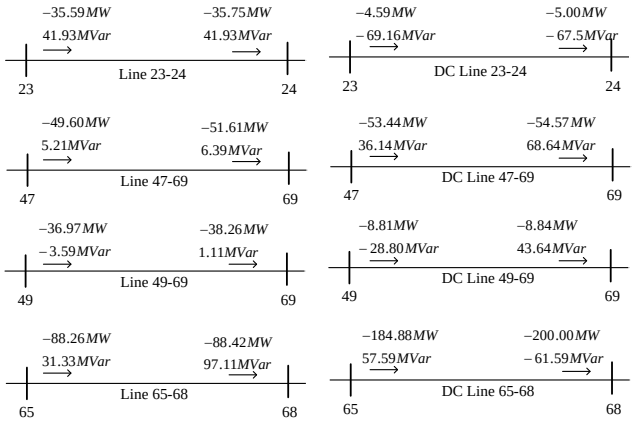

Fig. 7. AC flows (Case 2 on the left) and DC flows (Case 3 on the right)

TABLE X ZONAL OPERATING COSTS (BASE CASE)

	Zone 1 ($)	Zone 2 ($)	Zone 3 ($)	Total ($)
Case0	-	496,426.10	659,534.06	-
Case1	392,072.22	672,699.45	662,393.33	1,727,165.00
Case2	401,636.59	671,112.28	657,851.13	1,730,600.00
Case3	392,260.48	667,646.87	668,334.65	1,728,242.00

Case 4: When the possible outage of unit 47 is considered, the system state cannot be transferred to a new base case state by applying the UC solution in Case 2. Consequently, power flow violations appear and Benders cuts are generated to recalculate the UC solution in Case 2 (preventive actions). For instance, we observe that generating units 46 and 49 that were off in Case 2 are now committed to guarantee the system security. The difference in daily operation cost (i.e., $1,743,653-$1,730,600 = $13,053) is the cost of preventive action for maintaining the security when the outage of generating unit 47 is considered.

Case 5: This is a controllable contingency whereby corrective actions (i.e., ED based on physical ramping) will mitigate transmission violations. The total operating cost is $1,735,712 which is higher than that in Case 3.

V. Conclusions

A VSC-DC transmission system is integrated into SCUC which is solved by the Benders decomposition method. The efficiency of the proposed model is examined in the base case and in contingency cases. In addition, the comparison of VSC-DC and CSC-DC systems emphasizes that CSC-DC systems would require reactive power compensations at converter stations to guarantee the system security. The presented model will expand the security margin by introducing preventive and corrective actions and transferring the AC/DC contingency state to a new base case state in the event of outages. The VSC-DC transmission systems can successfully control active and reactive power flows, increase the transfer capability of AC transmission, mitigate AC flow congestions, decommit expensive generating units, and improve the operating costs in the base case and contingencies.

VI. References

[1] X. P. Zhang, "Multiterminal Voltage-Sourced Converter-Based DC Models for Power Flow Analysis," *IEEE Transactions on Power Systems*, Vol. 19, No. 4, pp. 1877-1884, Nov. 2004.

[2] R. L. Hendriks, J. H. D. Boon, G. C. Paap, W. L. Kling, "Connecting Offshore Wind Farms to (VSC-)DC Interconnections," *NORDIC Wind Power Conference*, May 2006.

[3] A. Lindberg, T. Larsson, "PWM and Control of Three Level Voltage Source Converters in an DC Back-to-Back Station," IEE proceeding on AC and dc Transmission, May 1996.

[4] M. P. Bahrman, J. G. Johansson, B. A. Nilsson, "Voltage Source Converter Transmission Technologies-The Right Fit for the Application," *IEEE Power Engineering Society General Meeting*, July, 2003.

[5] A. Lotfjou, M. Shahidehpour, Y. Fu, and Z. Li, "Security-Constrained Unit Commitment with AC/DC Transmission Systems," IEEE Transactions on Power System, vol. 25, no. 1, pp. 531-542, Feb 2010.

[6] M. Bahrman, M. Baker, J. Bowles, R. Bunch, J. Lemay, W. Long, J. McConnach, R. Menizies, J. Reeve, M. Szechtman, "Integration Of Small Taps Into (Existing) DC Links," *IEEE Transactions on Power Delivery*, Vol. 10, No.3 , pp. 1699-1706, July 1995.

[7] M. Aredes, C. Portela, F. C. Mechado, "A 25-MW Soft-Switching DC Tap for ±500-kV Transmission Lines," *IEEE Transactions on Power Delivery*, Vol. 19, No. 4, pp. 1835-1842, Oct. 2004.

[8] C. A. Camacho, O. L. Tortelli, E. Acha, C.R. F. Esquivel, "Inclusion of a high DC-Voltage Source Converter Model in a Newton-Raphson Power Flow Algorithm," *IEE Proceeding General Transmission Distribution*, Vol. 150, No. 6, Nov. 2003.

[9] L. Genyin, Z. Ming, H. Jie, L. Guangki, L. Haifeng, "Power Flow Calculation of Power Systems Incorporating VSC-DC," *IEEE International Conference On Power System Technology*, Singapore, Nov. 2005.

[10] X. Wei, J. H. Chow, B. Fardanesh, A. A. Edris, "A Common Modeling Framework of Voltage-Sourced Converters for Load Flow, Sensitivity, and Dispatch Analysis," *IEEE Transactions on Power Systems*, Vol. 19, No. 2, pp. 934-941, May 2004.

[11] A. Pizano-Martinze, C. R. Fuerte-Esquivel, H. Ambirz-Perez, E. Acha, "Modeling of VSC-Based DC Systems for a Newton-Raphson OPF Algorithm," *IEEE Transaction on Power System*, Vol. 22, No. 4, pp. 1794-1803, Nov. 2007.

[12] Y. Fu, M. Shahidehpour, Z. Li, "Security Constrained Unit Commitment with AC Constraints," *IEEE Transactions on Power Systems*, Vol. 20, No. 2, pp. 1001-1013, May 2005.

[13] G. Huang, S. C. Hsieh, "Fast Textured Algorithms for Optimal Power Delivery Problems in Restructured Environments," *IEEE Transactions on Power Systems*, Vol. 13, No. 2, pp. 493-500, May 1998.

[14] H. Saadat, "Power System Analysis," McGraw-Hill, 2002.

[15] M. Shahidehpour, H. Yamin, and Z. Y. Li, Market Operations in Electric Power Systems, Wiley, 2002.

[16] Y. Fu, M. Shahidehpour, and Z. Li, "AC contingency dispatch based on security-constrained unit commitment," *IEEE Transactions on Power System*, vol. 21, no. 2, pp. 897–908, May 2006.

VII. Biographies

Azim Lotfjou received his BS and MS in E.E. from Sharif University of Technology, Tehran, in 2001 and 2004, respectively. He completed his PhD degree in 2009 in the ECE Department at Illinois Institute of Technology.

Mohammad Shahidehpour (F'01) is Bodine Professor in the Electrical and Computer Engineering Department at Illinois Institute of Technology. He also serves as the Director of the Center for Electricity Innovation at IIT. He was the recipient of an honorary doctorate from the Polytechnic University of Bucharest in 2009.

Yong Fu (M'05) received his BS and MS in E.E. from Shanghai Jiaotong University, China, in 1997 and 2002, respectively and PhD degree in E.E. from Illinois Institute of Technology in 2006. Presently, he is an assistant professor in the ECE Department at Mississippi State University.

Appendix A: Jacobian Matrixes

The elements of Jacobian matrix $\mathbf{J}_1$ at the AC bus m connected to the DC converter h are formulated as

$$\frac{\partial \Delta P_{m,h}}{\partial V_{dc,h}} = -I_{dc,h} \tag{A.1}$$

$$\frac{\partial \Delta P_{m,h}}{\partial I_{dc,h}} = -V_{dc,h} \tag{A.2}$$

$$\frac{\partial \Delta Q_{m,h}}{\partial V_{m,h}} = -\frac{2V_{m,h} - E_h \cos(\phi_h)}{X_h} \tag{A.3}$$

$$\frac{\partial \Delta Q_{m,h}}{\partial E_h} = \frac{V_{m,h} \cos(\phi_h)}{X_h} \tag{A.4}$$

$$\frac{\partial \Delta Q_{m,h}}{\partial \varphi_h} = -\frac{V_{m,h} E_h \sin(\phi_h)}{X_h} \tag{A.5}$$

The elements of Jacobian matrix $\mathbf{J}_2$ at AC bus m connected to the DC converter h are formulated as

$$\frac{\partial \Delta R1_h}{\partial E_h} = 1 \tag{A.6}$$

$$\frac{\partial \Delta R1_h}{\partial M_h} = \begin{cases} -\dfrac{V_{dc,h}}{2\sqrt{2}} & \text{for rectifier} \\ \dfrac{V_{dc,h}}{2\sqrt{2}} & \text{for inverter} \end{cases} \tag{A.7}$$

$$\frac{\partial \Delta R1_h}{\partial V_{dc,h}} = \begin{cases} -\dfrac{M_h}{2\sqrt{2}} & \text{for rectifier} \\ \dfrac{M_h}{2\sqrt{2}} & \text{for inverter} \end{cases} \tag{A.8}$$

$$\frac{\partial \Delta R2_h}{\partial I_{dc,h}} = 1 \tag{A.9}$$

$$\frac{\partial \Delta R2_h}{\partial M_h} = \begin{cases} -\dfrac{V_{m,h} \sin(\phi_h)}{2\sqrt{2} X_h} & \text{for rectifier} \\ \dfrac{V_{m,h} \sin(\phi_h)}{2\sqrt{2} X_h} & \text{for inverter} \end{cases} \tag{A.10}$$

$$\frac{\partial \Delta R2_h}{\partial V_{m,h}} = \begin{cases} -\dfrac{M_h \sin(\phi_h)}{2\sqrt{2}X_h} & \text{for rectifier} \\ \dfrac{M_h \sin(\phi_h)}{2\sqrt{2}X_h} & \text{for inverter} \end{cases} \quad (A.11)$$

$$\frac{\partial \Delta R2_h}{\partial \phi_h} = \begin{cases} -\dfrac{M_h V_{m,h} \cos(\phi_h)}{2\sqrt{2}X_h} & \text{for rectifier} \\ \dfrac{M_h V_{m,h} \cos(\phi_h)}{2\sqrt{2}X_h} & \text{for inverter} \end{cases} \quad (A.12)$$

The partial derivatives of $\Delta R3_h$ will depend on the configuration of VSC-DC transmission system. For example, the partial derivatives of $\Delta R3_1$ for the two-terminal DC transmission system shown in Fig. 2 are listed as

$$\frac{\partial \Delta R3_1}{\partial I_{dc,1}} = 1, \frac{\partial \Delta R3_1}{\partial V_{dc,1}} = -\frac{1}{R_{dc}}, \frac{\partial \Delta R3_1}{\partial V_{dc,2}} = -\frac{1}{R_{dc}}$$

$$\frac{\partial \Delta R3_2}{\partial I_{dc,2}} = 1, \frac{\partial \Delta R3_2}{\partial V_{dc,1}} = -\frac{1}{R_{dc}}, \frac{\partial \Delta R3_2}{\partial V_{dc,2}} = -\frac{1}{R_{dc}}$$

The elements of Jacobian matrix $\mathbf{A}_2$ and $\mathbf{B}_2$ for the DC converter v are formulated as

$$\frac{\partial \Delta P_h}{\partial V_{dc,h}} = -I_{dc,h} \quad (A.13)$$

$$\frac{\partial \Delta P_h}{\partial I_{dc,h}} = -V_{dc,h} \quad (A.14)$$

The elements of Jacobian matrix $\mathbf{A}_3$, $\mathbf{B}_3$ and $\mathbf{C}_3$ for the DC converter v are formulated as

$$\frac{\partial \Delta Q_h}{\partial V_{m,h}} = -\frac{E_h \cos(-\phi_h)}{X_h} \quad (A.15)$$

$$\frac{\partial \Delta Q_h}{\partial E_h} = \frac{2E_h - V_h \cos(-\phi_h)}{X_h} \quad (A.16)$$

$$\frac{\partial \Delta Q_{m,h}}{\partial \varphi_h} = -\frac{E_h V_{m,h} \sin(-\phi_h)}{X_h} \quad (A.17)$$

Appendix B: Network data for 6-Bus system

TABLE B.I
BUS DATA

Bus No.	V_{Max} (pu)	V_{Min} (pu)
1	1.10	0.95
2, 3,4,5,6	1.15	0.90

TABLE B.II
TRANSMISSION LINE DATA

Line No.	From Bus	To Bus	R (pu)	X (pu)	Flow Limit (MW)
1	1	2	0.0050	0.170	150
2	1	4	0.0030	0.258	75
3	2	4	0.0070	0.197	100
4	5	6	0.0020	0.140	90
5	3	6	0.0005	0.018	90

TABLE B.III
TAP CHANGING TRANSFORMER DATA

Tap-Changing Transformers	From Bus	To Bus	X (pu)	Tap Max	Tap Min	Cap (MW)
T1	2	3	0.037	0.98	0.95	100
T2	4	5	0.037	0.98	0.95	90

TABLE B. IV
HOURLY LOAD

Hour	Pd (MW)	Qd (MVAR)	Hour	Pd (MW)	Qd (MVAR)
1	175.19	50.28	13	242.18	69.51
2	165.15	47.40	14	243.60	69.91
3	158.67	45.54	15	248.86	71.42
4	154.73	44.41	16	255.79	73.41
5	155.06	44.50	17	256.00	73.47
6	160.48	46.06	18	246.74	70.81
7	173.39	49.76	19	245.97	70.59
8	177.60	50.97	20	237.35	68.12
9	186.81	53.61	21	237.31	68.11
10	206.96	59.40	22	232.67	66.78
11	228.61	65.61	23	195.93	56.23
12	236.10	67.76	24	195.60	56.14

TABLE B.V
GENERATOR DATA

U	Bus No.	Unit Cost Coefficients			Pmax (MW)	Pmin (MW)	Qmax (MVAR)
		A (MBtu)	b (MBtu/MWh)	c (MBtu/MW^{2}h)			
G1	1	176.9	13.5	0.1	220	100	100
G2	2	176.9	17.6	0.1	100	10	50
G3	6	176.9	32.6	0.1	30	10	10

TABLE B.V
GENERATOR DATA (CONTUNIED)

Qmin (MVAR)	Ini. St. (h)	Min Down (h)	Min Up (h)	Ramp (MW/h)	Start Up (MBtu)	Fuel Price ($/MBtu)
-100	4	4	4	55	100	1.2469
-40	2	2	3	50	200	1.2461
-10	1	1	1	20	0	1.2462

TABLE B.VI
CONVERTERS DATA FOR THE TWO-TERMINAL DC SYSTEM

Type	X (pu)	P_{min} (MW)	P_{max} (MW)	Q_{min} (MVAR)	Q_{max} (MVAR)
Rec.	0.02	0	150	-70	70
Inv.	0.02	0	150	-70	70

TABLE B.VI
CONVERTERS DATA FOR THE TWO-TERMINAL DC SYSTEM (CONTINUFES)

E_{min} (pu)	E_{max} (pu)	$V_{dc,min}$ (pu)	$V_{dc,max}$ (pu)
0.85	1.15	0.85	1.2
0.85	1.15	-1.2	-0.85

TABLE B.VII
STATIC LOAD DISTRIBUTION FACTORS

L1	L2	L3
0.1	0.2	0.2